AD-A043 549 NAVAL RESEARCH LAB WASHINGTON D C F/G 9/2
EXPLICIT CHEBYCHEV-ITERATIVE SOLUTION OF NONSELF-ADJOINT ELLIPT--ETC(U)
JUN 77 B E MCDONALD

UNCLASSIFIED NRL-MR-3541 NL

| OF |
AD
A043549

END
DATE
FILMED
9 -77
DDC

AD A043549

NRL Memorandum Report 3541

Explicit Chebychev-Iterative Solution of Nonself-Adjoint Elliptic Equations on a Vector Computer

B. E. McDONALD

Plasma Dynamic Branch
Plasma Physics Division

June 1977

DDC
RECEIVED
AUG 30 1977
B

NAVAL RESEARCH LABORATORY
Washington, D.C.

Approved for public release; distribution unlimited.

AD No.
DDC FILE COPY

SECURITY CLASSIFICATION OF THIS PAGE (When Data Entered)

REPORT DOCUMENTATION PAGE

READ INSTRUCTIONS BEFORE COMPLETING FORM

1. REPORT NUMBER: NRL Memorandum Report 3541

2. GOVT ACCESSION NO.

3. RECIPIENT'S CATALOG NUMBER

4. TITLE (and Subtitle): EXPLICIT CHEBYCHEV-ITERATIVE SOLUTION OF NONSELF-ADJOINT ELLIPTIC EQUATIONS ON A VECTOR COMPUTER.

5. TYPE OF REPORT & PERIOD COVERED: Interim report on a continuing NRL problem.

6. PERFORMING ORG. REPORT NUMBER

7. AUTHOR(s): B.E. McDonald

8. CONTRACT OR GRANT NUMBER(s)

9. PERFORMING ORGANIZATION NAME AND ADDRESS: Naval Research Laboratory, Washington, D.C. 20375

10. PROGRAM ELEMENT, PROJECT, TASK AREA & WORK UNIT NUMBERS: NRL Problem A03-16 and H02-27B; Subtask PR033-02-42-5308; DNA Subtask S99QAXHC041

11. CONTROLLING OFFICE NAME AND ADDRESS: Office of Naval Research, Arlington, Virginia 22217

12. REPORT DATE: June 1977

13. NUMBER OF PAGES: 47

14. MONITORING AGENCY NAME & ADDRESS (if different from Controlling Office): NRL-MR-3541

15. SECURITY CLASS. (of this report): UNCLASSIFIED

15a. DECLASSIFICATION/DOWNGRADING SCHEDULE

16. DISTRIBUTION STATEMENT (of this Report)

Approved for public release; distribution unlimited.

17. DISTRIBUTION STATEMENT (of the abstract entered in Block 20, if different from Report)

DDC
RECEIVED
AUG 30 1977
B

18. SUPPLEMENTARY NOTES

19. KEY WORDS (Continue on reverse side if necessary and identify by block number)

Complex eigenvalues
Partial differential equations
nonsymmetric operators
Iterative solution
Chebychev polynomials
Pipeline computers

20. ABSTRACT (Continue on reverse side if necessary and identify by block number)

The Chebychev explicit method[1] can be extended to nonsymmetric matrices L whose complex eigenvalues lie with an ellipse of a particular type in the complex plane. The vectorizability of the method results in high execution efficiency on a "pipeline" computer. We derive the method and its convergence rate, and give a comparison with an ADI solution. The comparison is taken from a 2D plasma turbulence code,[5,6] in which $L = \nabla^2 + \underset{\sim}{A}(x,y)\cdot\underset{\sim}{\nabla}$. The explicit method is approximately 3 times more efficient than ADI for the model problem solved on a two-pipe Texas Instruments ASC. The method has been used successfully on meshes of 34 × 34, 50 × 50, and 130 × 130 points.

DD FORM 1 JAN 73 1473 EDITION OF 1 NOV 65 IS OBSOLETE
S/N 0102-014-6601

SECURITY CLASSIFICATION OF THIS PAGE (When Data Entered)

251950

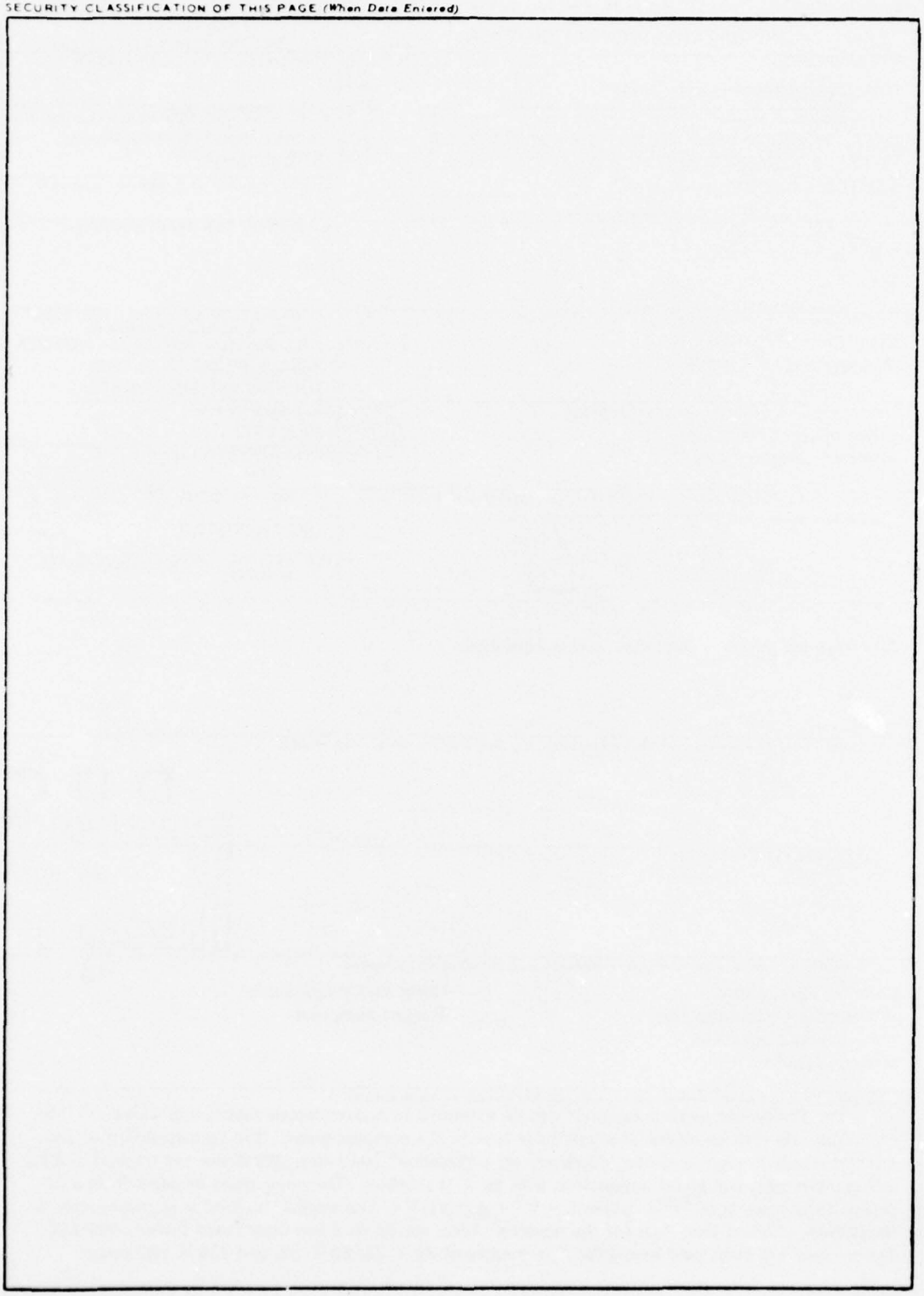

CONTENTS

ACCESSION for
NTIS White Section ☑
DDC Buff Section ☐
UNANNOUNCED ☐
JUSTIFICATION
BY
DISTRIBUTION/AVAILABILITY CODES
Dist. and/or SPECIAL
A

EXPLICIT CHEBYCHEV-ITERATIVE SOLUTION OF NONSELF-ADJOINT ELLIPTIC EQUATIONS ON A VECTOR COMPUTER

Introduction

The computational mathematics literature is well stocked with numerical methods for solution of self-adjoint linear operator equations. See, for example, the many methods and references given by Varga,[2] Birkhoff,[2] and Vichnevetsky.[3] However, many fewer approaches are offered for nonself adjoint problems. One occasionally encounters the suggestion that the equation $L(\underset{\sim}{r})\phi(\underset{\sim}{r}) = S(\underset{\sim}{r})$ (with L the linear operator, and S the known driving term) be made self adjoint by an extra application of the adjoint of L: $L^{\dagger}L\phi = L^{\dagger}S$. There may be cases in which this approach has merit. However, it has two immediate drawbacks: (1) one has to work with a higher order equation, and (2) the ratio of maximum to minimum eigenvalue amplitude, an indicator of the amount of numerical work required, is squared. There are situations in which it may be desirable to transform a self-adjoint problem into a nonself-adjoint one. For example, in a heat conduction problem, L contains the operator $\underset{\sim}{\nabla}\cdot K\underset{\sim}{\nabla}$, where K is the thermal conductivity. If K varies greatly in magnitude, the eigenvalue span of L will be increased accordingly, making the numerical solution more difficult. A possible remedy is to divide through by K, so that L contains the nonself adjoint operator $\nabla^2 + \underset{\sim}{\nabla} \log K\cdot\underset{\sim}{\nabla}$.

An approach that has gained recent attention is a combination of approximate factorization and the conjugate gradient method. See Vichnevetsky,[3] p. 60, or Meijerink and van der Vorst.[4] With some adaptation, this approach may hold promise for nonself-adjoint problems.

Note: manuscript submitted June 13, 1977.

But the factorization stage is awkward for vector computers. One must solve upper-and lower-triangular matrix equations, which resemble recursion formulas. As a result, the computer must initiate and complete certain calculations one at a time, rather than doing several in parallel. Thus we wish to offer an alternative method which allows complete vectorization (parallel processing) for all interior mesh points of a multidimensional grid. This method is a generalization of the Chebychev semi-iterative method (Varga,[1] Chap. 5).

Assumptions

We seek an iterative solution to the equation

$$L\phi = S, \tag{1}$$

where S is a known source vector, and L is a matrix or finite difference operator. We assume L has complex eigenvalues $\lambda_r + i\lambda_i$, with all λ_r being of the same sign. We also assume all λ fall within an ellipse in the complex plane (see Fig. 1) whose major axis coincides with the real axis. The intersections of the ellipse with the real axis are b - a and b + a, with

$$b/a > 1. \tag{2}$$

The semiminor axis of the ellipse is c. We require

$$c < |a|, \text{ and thus} \tag{3}$$

$$\lambda_{i_{max}} - \lambda_{i_{min}} < \lambda_{r_{max}} - \lambda_{r_{min}}. \tag{4}$$

We assume that (1) possesses an exact solution Φ. At the end of n iterations, we will have an approximate solution ϕ^n, whose error is defined to be

$$\epsilon^n = \phi^n - \Phi. \tag{5}$$

The iterative method is to be such that

$$\epsilon^n = P_n(L)\epsilon^o, \tag{6}$$

where P_n is a polynomial of degree n. Substitution of (5) into (6) gives

$$\phi^n = P_n(L)\phi^o - (P_n(L) - 1)\Phi. \tag{7}$$

We do not know Φ in advance, but we do know $L^k\Phi = L^{k-1}S$ for $k > 0$. Thus from (7) we must require that the zero-degree term of $P_n(L)$ be 1:

$$P_n(0) = 1. \tag{8}$$

We wish to choose P_n such that its magnitude is as small as possible everywhere within the ellipse containing eigenvalues of L.

Determination of P_n for a Real Min-Max Problem

The problem of minimizing the maximum value of $|P_n(x)|$ subject to $P_n(0) = 1$ has a well known solution when x is restricted to real values between b - a and b + a with $b/a > 1$. The standard argument points out that the desired P_n is such that all maxima of $|P_n|$ have the same value. One immediately determines that P_n is proportional to a Chebychev polynomial The Chebychev polynomials T_n are such that

$$T_n(\cos \alpha) = \cos n\alpha, \quad \text{and}$$

$$T_n(\cosh \alpha) = \cosh n\alpha. \tag{9}$$

That $\cos n\alpha$ is a polynomial in $\cos \alpha$ results from the elementary identity

$$\cos(m + 1)\alpha = 2 \cos \alpha \cos m\alpha - \cos(m - 1)\alpha. \tag{10}$$

Equation (10) is also valid when cosh is substituted for cos. Thus if $\cos m\alpha$ and $\cos(m - 1)\alpha$ are polynomials in $\cos \alpha$, then so is $\cos(m + 1)\alpha$. This is the case for $m = 0$ and 1, so it is also true for all $m > 0$. Equation (10) also gives the recursion formula for the Chebychev polynomials:

$$T_{m+1}(x) = 2 x T_m(x) - T_{m-1}(x). \tag{11}$$

From (9) we can see that $|T_n(x)|$ reaches a limiting value of 1 n + 1 times as x varies from -1 to 1. Thus the solution to the min-max problem for real x is

$$P_n(x) = T_n\left(\frac{x-b}{a}\right) / T_n\left(-\frac{b}{a}\right), \tag{12}$$

and

$$|P_n|_{max} = \left|T_n\left(-\frac{b}{a}\right)\right|^{-1} \tag{13}$$

$$= 1/\cosh\left(n \cosh^{-1}\left(\frac{b}{a}\right)\right) < 1.$$

Determination of P_n for a Complex Min-Max Problem

Slightly less well known is the fact that the Chebychev polynomials also satisfy the following problem: With

$$z = \xi + i\eta \tag{14}$$

find $P_n(z)$ such that $P_n(0) = 1$, and such that every maximum of $|P_n(z)|$ on the ellipse

$$\left(\frac{\xi - b}{a}\right)^2 + \frac{\eta^2}{c^2} \leq 1 \tag{15}$$

has the same value.

Let us now consider the behavior of the Chebychev polynomials in the complex plane. It is convenient to express ξ and η in terms of dimensionless variables ξ', η', α and β as follows:

$$\begin{aligned} \xi &= \lambda_o \xi' \\ \eta &= \lambda_o \eta' \\ \xi' &= \cos\alpha \cosh\beta \\ \eta' &= \sin\alpha \sinh\beta. \end{aligned} \tag{16}$$

Here λ_o is a dimensional quantity of arbitrary magnitude having the same dimensions as the operator L. Let us first demonstrate that arbitrary ξ' and η' can be expressed as in (16) with real α and β. One can eliminate $\cos\alpha$ from (16) and obtain the following equation for $\cosh\beta$:

$$F(u) \equiv u^2 - u(\xi'^2 + \eta'^2 + 1) + \xi'^2 = 0, \tag{17}$$

where $u = \cosh^2 \beta$. Incidentally, one obtains the same equation by eliminating cosh β and setting $u = \cos^2 \alpha$. Note from (17) that

$$F(0) = \xi'^2$$

$$F(1) = -\eta'^2, \text{ and}$$

$$F(\xi'^2 + \eta'^2 + 1) = \xi'^2.$$

We see immediately that there must be one real root $0 \leq u_1 \leq 1$ and another real root $1 \leq u_2 \leq 1 + \xi'^2 + \eta'^2$. The lesser of the two roots can be taken to be $\cos^2 \alpha$, and the greater to be $\cosh^2 \beta$, with α and β both real. The signs of ξ' and η' can be adjusted properly by proper choice of the sign of β and phase of α modulo π.

Let us return to (16) and define

$$\begin{aligned} z' &= \xi' + i\eta' \\ &= \cos \alpha \cosh \beta + i \sin \alpha \sinh \beta \\ &= \cos (\alpha + i\beta). \end{aligned} \tag{19}$$

From (9) and (19) we have

$$\begin{aligned} T_n(z') &= \cos(n\alpha + in\beta) \\ &= \cos n\alpha \cosh n\beta + i \sin n\alpha \sinh n\beta. \end{aligned} \tag{20}$$

From (20) we find with only a slight amount of algebra

$$|T_n(z')|^2 = \cos^2 n\alpha + \sinh^2 n\beta. \tag{21}$$

We can see from (16) that surfaces of constant β are ellipses in $\xi' - \eta'$ space:

$$\xi'^2 + (\eta'/\tanh \beta)^2 = \cosh^2 \beta. \tag{22}$$

With β fixed, one can see from (16) that the point (ξ', η') scans once around the ellipse as α varies from 0 to 2π. Thus (21) shows that $|T_n(z')|$ reaches the same maximum value 2 n times as z' scans around the perimeter of the ellipse of constant β.

It remains only to show that no maxima occur in the interior of the ellipse (22). We can conclude this from the fact that $T_n(z')$ has n distinct real roots:

$$T_n(z') = K_n \prod_{m=1}^{n} \left(z' - \cos \frac{(m - 1/2)\pi}{n} \right), \tag{23}$$

where K_n is a normalization coefficient. Thus

$$|T_n(z')|^2 = K_n^2 \prod_{m=1}^{n} \left(\left(\xi' - \cos \frac{(m - 1/2)\pi}{n} \right)^2 + \eta'^2 \right) . \tag{24}$$

This shows that $|T_n(z')|$ increases monotonically away from the real axis ($\eta' = 0$), and thus there are no local maxima. Thus all maxima in the region enclosed by the ellipse (22) must occur on the boundary. As pointed out by (21), these maxima of $|T_n(z')|$ all have the same value. Therefore we conclude that the Chebychev polynomials solve the problem stated just prior to (15).

In order to put the ellipse (15) into the form (22), set

$$\begin{aligned} \xi &= b + af\xi' \\ \eta &= af\eta' \end{aligned} \tag{25}$$

where f is a dimensionless number yet to be specified. Substitution of (25) into (15) gives for the perimeter of the ellipse

$$\xi'^2 + (\eta' a/c)^2 = f^{-2} \ . \tag{26}$$

Thus from (22) we take

$$\begin{aligned} \beta &= \tanh^{-1} c/a \\ f &= 1/\cosh \beta \\ &= (1 - c^2/a^2)^{1/2}. \end{aligned} \tag{27}$$

The desired polynomial is proportional to $T_n(\xi' + i\eta')$, and in fact is

$$P_n(z) = T_n\left(\frac{z - b}{fa}\right) \Big/ T_n\left(-\frac{b}{fa}\right) \ . \tag{28}$$

Note that in the limit $c \to 0$, we have $f \to 1$, and $z \to \xi$. In this limit the complex solution (28) reduces to the real solution (12) as it should.

What maximum amplitude is attained by (28)? From (21) we find for the ellipse of constant β

$$\begin{aligned} |T_n(z')|_{max} &= (1 + \sinh^2 n\beta)^{1/2} \\ &= \cosh n\beta. \end{aligned} \tag{29}$$

Substituting this into (28) gives

$$|P_n(z)|_{max} = \frac{T_n(\cosh \beta)}{T_n(b/a \cosh \beta)} < 1, \qquad (30)$$

where β is given in (27). We have dropped the minus sign from the argument of the denominator of (28) because $T_n(x)$ is an even or odd function of x when n is even or odd respectively. We know (30) is less than 1 because the argument in the denominator is larger than that in the numerator and $T_n(x)$ is monotonically increasing for $x > 1$, as one can show from (9).

Construction of the Iterative Method

We shall take the polynomial of (28) to be the proper choice for use in constructing the approximate solution to (1) according to (7). We must choose between two approaches for generating the polynomial $P_n(L)$. The first is factorization of P_n into n linear factors. We have tried this approach and found it subject to roundoff error amplification. The reason for this is that the process is equivalent to n overrelaxation steps, some of which reduce the long wavelength errors at the expense of increasing the short wavelength errors. The short wavelength errors are eventually brought back down, but any roundoff error introduced while they were large tends to contaminate the final result.

The second and more preferable approach to constructing $P_n(L)$ is through the use of a recursion formula. The only possible drawback to this method is that one extra array of storage is required for retention of earlier iterates. We substitute (28) into (7) to obtain

$$\phi^{n+1} = \frac{T_{n+1}\left(\frac{L-b}{fa}\right)(\phi^{\circ} - \Phi)}{T_{n+1}\left(-\frac{b}{fa}\right)} + \Phi \quad . \tag{31}$$

In the numerator of this expression let us express T_{n+1} in terms of T_n and T_{n-1} according to the recursion formula (11), and then express T_n and T_{n-1} in terms of ϕ and ϕ^{n-1} according to (31). Let us define

$$q = -\frac{b}{fa} \tag{32}$$

$$= -b/\sqrt{a^2 - c^2}$$

and use $L\Phi = S$.

Then we find

$$\phi^{n+1} = \frac{1}{T_{n+1}(q)} \left[2T_n(q)/fa((L - b)\phi^n - S) - T_{n-1}(q)\phi^{n-1}\right]$$

$$+ \Phi \left[1 + (-2\, qT_n(q) + T_{n-1}(q))/T_{n+1}(q)\right]. \tag{33}$$

Notice that the coefficient of Φ is zero by (11). Recall that we imposed this condition at the outset in (8).

In order to use this method we must know the first two terms in the recursion. We get these by direct construction of $P_n(L)$, and obtain

$$\phi^{\circ} = \text{arbitrary trail solution} \tag{34}$$

$$\phi^1 = \phi^{\circ} - 1/b\ (L\phi^{\circ} - S)$$

$$\phi^{n+1} = \frac{2\,T_n(q)}{T_{n+1}(q\sqrt{a^2 - c^2}} ((L - b)\phi^n - S)$$

$$- \frac{T_{n-1}(q)}{T_{n+1}(q)} \phi^{n-1}, \quad n > 0.$$

Error Estimates

If B is an eigenvector of L such that

$$LB = \lambda B, \tag{35}$$

where λ is a complex constant, then

$$P_n(L)B = P_n(\lambda)B. \tag{36}$$

Let us imagine that the error ϵ^0 of (5) is expressed as a linear combination of the eigenvectors of L. We have assumed all eigenvalues of L to lie within an ellipse (15) in the complex plane. Then from (6), (27) and (30), the coefficients of the eigenvector expansion of ϵ^n have each been decreased in amplitude by at least a factor

$$|P_n(\lambda)| \leq E_n(a,b,c) \equiv T_n(a/\sqrt{a^2-c^2})/T_n(b/\sqrt{a^2-c^2}). \tag{37}$$

In Fig. 2 we plot this error limit as a function of n for various values of the ratio of maximum to minimum real eigenvalue,

$$R \equiv \frac{b+a}{b-a} \ , \tag{38}$$

and ellipse axis ratio c/a. One notices that the error limit decreases approximately exponentially with n, and that the rate of decrease depends strongly on R. In practice, when R is greater than about 10^3, we use a filtering process to be described later to bring down the effective value of R. The slow convergence at large R is due to the fact that one is attempting to reduce the error by a diffusion process, which is slow for long wavelengths.

Let us derive an approximate expression for (37) in the limit of large R. It is convenient to define

$$\begin{aligned} \delta &= b/a - 1 \\ &= 2/(R - 1), \text{ and} \\ \rho &= c/a. \end{aligned} \tag{39}$$

From (9) and the identity,

$$\cosh^{-1} x = \log \left(x + \sqrt{x^2 - 1}\right) \tag{40}$$

we have

$$E_n = \frac{\cosh (n \log Q_1)}{\cosh (n \log Q_1 + n \log Q_2)} \tag{41}$$

$$= 1/[\cosh(n \log Q_2) + \tanh(n \log Q_1) \sinh(n \log Q_2)]$$

where

$$Q_1 = \frac{1 + \rho}{\sqrt{1 - \rho^2}} \tag{42}$$

$$Q_2 = \frac{1 + \delta + \sqrt{2\,\delta + \delta^2 + \rho^2}}{1 + \rho} \quad .$$

Since Q_1 and Q_2 are both greater than 1, (41) yields

$$2 \exp(-n \log Q_2) > E_n > \exp(-n \log Q_2). \tag{43}$$

Thus the estimate

$$E_n \approx \sqrt{2} \left(\frac{1 + \delta + \sqrt{2\,\delta + \delta^2 + \rho^2}}{1 + \rho} \right)^{-n} \tag{44}$$

is always correct within a factor of $\sqrt{2}$. Defining the convergence rate to be

$$C \equiv -\partial \log E_n / \partial n, \tag{45}$$

we can find simple expressions for C in the limit $\delta \ll 1$. For $\rho \ll \delta$, $C \approx \sqrt{2\,\delta}$. When $\rho \gg \delta$, then $C \approx \delta/\rho$. This shows that convergence slows down when the eigenvalues of the operator L have significant imaginary parts.

Application to a Model Problem

As a test of the method (33) - (34) and the error estimate (37) we shall solve numerically the two dimensional equation

$$\nabla^2 \phi + \underset{\sim}{A}(x,y) \cdot \nabla \phi = S(x,y), \tag{46}$$

on a rectangular grid with constant mesh spacing subject to doubly periodic boundary conditions. Equations of this form arise in plasma physics when charge neutrality is imposed upon a plasma with a non-isotropic electrical conductivity, with ϕ being the electrostatic

potential. For an application to the earth's ionosphere, see McDonald, et al.[5,6] Another physical situation in which an equation of the form (46) arises is that of a steady state distribution of a tracer element or pollutant ϕ in a given wind field subject to known diffusion and production-loss rates.

The mesh is assumed to be K_x by K_y interior mesh points. We choose the x direction so that

$$K_x \geq K_y. \tag{47}$$

We also assume the mesh intervals to be

$$\delta x = \delta y = \text{constant} \tag{48}$$

We use redundant guard cells around the perimeter of the mesh for efficient handling of the boundary conditions. This results in a complete mesh of $(K_x + 2) \times (K_y + 2)$ points. We use second order 5 point representation of the derivatives in (46):

$$\begin{aligned} L\phi_{IJ} \equiv\ & (\phi_{I+1,J} + \phi_{I-1,J} + \phi_{I,J+1} \\ & + \phi_{I,J-1} - 4\,\phi_{IJ})/\delta x^2 \\ & + AX_{IJ}(\phi_{I+1,J} - \phi_{I-1,J})/2\,\delta x \\ & + AY_{IJ}(\phi_{I,J+1} - \phi_{I,J-1})/2\,\delta x. \end{aligned} \tag{49}$$

Here I and J are the x and y mesh point indices, and AX and AY are the x and y components of $\underset{\sim}{A}$ respectively.

In order to estimate the eigenvalues of L it is necessary to consider $\underset{\sim}{A}$ constant. Then the eigenfunctions are complex exponentials,

$$\phi_{\underset{\sim}{k}} = \exp\left(2\pi i\left(\frac{k_x I}{K_x} + \frac{k_y J}{K_y}\right)\right), \tag{50}$$

where $k_x = 0, 1, 2, \ldots K_x - 1$, etc. for k_y. (51)

The eigenvalues are

$$\lambda_{\underset{\sim}{k}} = \frac{2}{\delta x^2}\left(\cos\frac{2\pi k_x}{K_x} + \cos\frac{2\pi k_y}{K_y} - 2\right) + i\left(\frac{AX}{\delta x}\sin\frac{2\pi k_x}{K_x} + \frac{AY}{\delta x}\sin\frac{2\pi k_y}{K_y}\right). \tag{52}$$

Construction of the Ellipse

In order to show that these eigenvalues lie within an ellipse in the complex plane, let us adopt the following abbreviated notation:

$$c_x = \cos\frac{2\pi k_x}{K_x} \tag{53}$$

$$s_x = \sin\frac{2\pi k_x}{K_x}$$

$$a_x = AX\delta x, \text{ etc. for } y.$$

Let $\xi' = c_x + c_y$ (54)

$$\eta' = a_x s_x + a_y s_y.$$

Let us consider the function

$$h(\xi', \eta') = \left(\frac{\xi'}{2}\right)^2 + \theta\left(\frac{\eta'}{\bar{a}}\right)^2, \tag{55}$$

where $\bar{a} = (a_x^2 + a_y^2)^{1/2}$, (56)

and θ is a tuning parameter to be determined later. Let us choose a_x and a_y so as to maximize (55). Then

$$h \leq 1/4\ (c_x + c_y)^2 + r\theta(s_x^2 + s_y^2) \tag{57}$$

$$= 1 - 1/4\ (c_x - c_y)^2 - (1/2 - r\theta)(s_x^2 + s_y^2),$$

where $$r = 1\ . \tag{58}$$

We shall carry r as a variable in the analysis, since, if we had averaged h over all possible orientations of the vector $\underset{\sim}{A}$, we would have had $r = 1/2$. It may not be necessary in every case to constrain the method to handle a few "unfortunate" orientations of $\underset{\sim}{A}$ (which happen to be resonant directions for the lowest few modes in the system). In general, $\underset{\sim}{A}$ will vary in space, so any destabilizing resonance will be localized.

Let us remove from consideration the modes $(k_x,k_y) = (0,0)$ and $(K_x/2,\ K_y/2)$. These are the mean value and odd-even mode components of ϕ. The mean value has no effect upon (47), and the odd-even mode can be removed straightforwardly. Then the lowest mode of consequence is $(k_x,k_y) = (1,0)$, for which

$$s_x \approx 2\pi/K_x, \quad K_x \gg 1, \tag{59}$$

$$s_y = 0.$$

To lowest order in s_x, (57) gives

$$h_{max} = 1 - \sigma^2(1/2 - r\theta), \quad \text{where} \tag{60}$$

$$\sigma^2 = (s_x^2 + s_y^2)_{min} = \left(\frac{2\pi}{K_x}\right)^2 . \tag{61}$$

We shall retain σ as a variable since it contains all relevant boundary condition information. Let us now express ξ' and η' in terms of the real and imaginary parts of $\lambda_{\underset{\sim}{k}}$ in (52). Then (55) becomes

$$\left(\frac{\lambda_r + 4/\delta x^2}{4/\delta x^2}\right)^2 + \theta\left(\frac{\lambda_i \delta x^2}{\bar{a}}\right)^2 \leq h_{max} \tag{62}$$

Comparing (62) and (15), we find the ellipse parameters

$$a = 4\, h_{max}^{1/2} /\delta x^2 \tag{63}$$

$$b = 4/\delta x^2$$

$$c = \theta^{-1/2}\, \bar{a} h_{max}^{1/2} /\delta x^2 .$$

Note we have removed inconsequential minus signs from (63). From (39) and (63)

$$\delta = h_{max}^{-1/2} - 1 \tag{64}$$

$$\approx 1/4\, \sigma^2(1 - 2\, r\theta).$$

Also

$$c/a = \rho = \bar{a}/4\, \theta^{-1/2}. \tag{65}$$

Maximizing the Convergence Rate

The expressions (64) and (65) for δ and ρ allow the error estimate (44) to be expressed in terms of θ. Maximizing the convergence rate then is equivalent to maximizing Q_2 in (42) with respect to θ. A straightforward approach of setting $\partial Q_2/\partial\theta = 0$ requires solution of a seventh degree polynomial. A much more satisfactory approach emerges when one replaces (42) with an approximate expression valid for $\delta \ll 1$:

$$Q_2 \approx 1 + \sqrt{2\,\delta + \rho^2} - \rho. \tag{66}$$

Equation (66) gives correct results to lowest order in δ for all $\rho \geq 0$. Denoting differentiation with respect to θ by prime, the condition for maximum Q_2 in (66) is

$$2\,\delta\rho'^2 = \delta'^2 + 2\,\rho\delta'\rho'. \tag{67}$$

Substituting from (64) and (65), we have

$$r^3\theta^3 + \mu^2(3\,r\theta - 1/2) = 0, \tag{68}$$

where

$$\mu = \frac{\bar{a}}{4\,\sigma}\, r^{1/2} = \frac{|\underset{\sim}{A}|K_x\delta x}{8\pi}\, r^{1/2}. \tag{69}$$

Equations (69) reflect the general result that μ and thus θ are independent of the number of cells into which the rectangular region is partitioned, provided $\delta x = \delta y$, and K_x, $K_y \gg 2\pi$.

We know that (68) has only one real root, since the derivative of (68) is never zero for real θ.

This root is

$$r\theta = (\mu^2/4)^{1/3} \left\{ (\sqrt{16\ \mu^2 + 1} + 1)^{1/3} - (\sqrt{16\ \mu^2 + 1} - 1)^{1/3} \right\} .$$

The solution to (68) has the limiting forms

$$r\theta \approx \left(\frac{\mu^2}{2}\right)^{1/3} , \quad \mu \ll 1 \tag{71}$$

$$r\theta \approx \frac{1}{6} , \quad \mu \gg 1$$

One can show fairly easily that θ varies monotonically with μ between these two limits. This behavior is verified in Fig. 3, in which $r\theta$ is plotted vs μ.

Convergence Rates for Small and Large $|\underset{\sim}{A}|$

Taking into consideration (42), (44), (45), and (66), we have the approximate convergence rate

$$C \approx \sqrt{2\ \delta + \rho^2} - \rho. \tag{72}$$

We can use (64), (65), and (70) to express (72) in terms of μ. The result is

$$C \approx \sigma/\sqrt{2}\ C_o(\mu), \quad \text{where} \tag{73}$$

$$C_o(\mu) = \sqrt{2} \left[\sqrt{1/2 - r\theta + \mu^2/r\theta} - \mu/\sqrt{r\theta} \right] . \tag{74}$$

Recall that $\sigma = 2\pi/K_x$ for doubly periodic boundaries. The dependence of C_o upon μ is shown in Fig. 4. Also plotted in Fig. 4 (dashed line) is the approximation

$$C_o(\mu) \approx (9.5\,\mu + 1)^{-1} \quad . \tag{75}$$

Using (71), we find the following limiting forms for C:

$$C \approx \sigma/\sqrt{2}\,(1 - 3\,(\mu^2/2)^{1/3}), \quad \mu \ll 1 \tag{76}$$

$$C \approx \sigma\mu^{-1}/6\sqrt{6} \quad , \quad \mu \geq 1.$$

This shows that as μ increases from 0 to 1, the convergence rate drops by approximately a factor of 10.

Removal of Long Wavelength Error on Coarse Grid

We can see from (61) and (73) that the number of iterations required to reach a certain level of error reduction is proportional to K_x. Thus the total number of operations required is proportional to $K_x^2 K_y$. Therefore it is advantageous to correct the long wavelength components of the solution on a coarse mesh, and interpolate onto a fine mesh before completing the solution. The interpolation introduces truncation error into the solution, so that the error estimates derived earlier may not hold on the large mesh. For this reason, it is best to alternate between large and small meshes more than once, attempting only a modest error reductions with each pass. In practice, use of a coarse grid becomes important for $K_x \geq 64$. For a grid of 128 x 128 interior points, a coarse grid of 32 x 32 interior points is used. First, the residual $L\phi^o - S$ is extracted on the fine grid. Then this

residual and $\underset{\sim}{A}$ are defined on the coarse grid using block averages of 16 fine grid points per coarse grid point. The coarse grid potential correction is initialized to zero and a large number of iterations are performed. Typically we use three times as many iterations on the coarse grid as on the fine grid. Then the potential correction is defined on the fine grid using bilinear interpolation, and the result is subtracted from ϕ^0. Then iterations are performed on the fine grid, making no attempt to make significant improvements in the lowest 5 to 10 modes of the solution. That is, we arbitrarily increase σ in (61) by a factor of 5 to 10. This results in improved convergence of the higher modes. The effectiveness of this fine grid-coarse grid approach may be improved significantly in a time dependent problem by two-level extrapolation for the trial solution ϕ^0.

Numerical Results

As a test of the iterative procedure (33) - (34) and the convergence estimate (73) we have solved (46) on meshes of 32 x 32 and 48 x 48 interior grid points without regridding; and on a 128 x 128 mesh with a reduced mesh of 32 x 32 interior points. All tests used doubly periodic boundary conditions. The numerical convergence rate comparisons were carried out as follows. Arbitrary forms were adopted for $\underset{\sim}{A}$ and a reference solution Φ. Then a source term was generated from Φ numerically using the difference operation (49). This source term was used in the iteration (33) - (34), with the approximate solution being initialized to zero. After a large number N of iterations (usually N = 40), a relative error E was defined to be the root mean square

residual of (46) divided by the root mean square of the source, S. The average convergence rate was then taken to be - log E/N.

In all cases convergence was fast enough to be consistent with (73), and in most cases was faster than (73). The one case in which convergence was just equal to (73) for all μ was for $\Phi_{IJ} = \sin 2\pi I/K_x$, and A_x = constant, $A_y = 0$. This is consistent with the discussion following (58). For determining μ in (69), we used the root mean square value for $|\underset{\sim}{A}|$, and r = 1.

Figure 5 shows convergence rates per second of computer time, - log E/t, obtained using a two pipe Texas Instruments ASC to solve the same set of problems with the Chebychev explicit method (CE) (upper curve) and with an alternating direction implicit method (ADI) (lower curve). These comparisons were made on a 50 x 50 mesh using data from the EJET plasma turbulence code.[5,6] The ADI solution used logarithmically spaced iteration parameters[5] and a partially vectorized tridiagonal solver.[5] Although ADI converged faster per iteration, the limited vectorizability of the method resulted in slow execution. Thus the result in Fig. 5 is machine dependent. The execution times per iteration were 25.8 milliseconds for ADI and 1.32 milliseconds for the Chebychev explicit method. To illustrate the computational efficiency of the explicit method, the lower limit on execution time per iteration (neglecting overhead and boundary value resetting) would be (48 x 48 interior points) x (11 operations per point) x (40 nanoseconds per operation) = 1.01 milliseconds. Thus the explicit method runs at 76% efficiency on a modest 50 x 50 mesh. ADI could be made more competitive

by the use of cyclic reduction rather than tridiagonal solution in the integration direction, but it is unlikely that any improvement would bring the convergence rate per second up to that of the explicit method. In addition, the boundary conditions are much easier to change in the explicit method than in the implicit one.

Acknowledgment

This work was supported by the Office of Naval Research and the Defense Nuclear Agency.

References

1. R. S. Varge, Matrix Iterative Analysis, Prentice-Hall, Englewood Cliffs, N.J. (1962).

2. Birkhoff, G., "The Numerical Solution of Elliptic Equations," Regional Conference Series in Applied Mathematics, SIAM, Philadelphia (1971).

3. R. Vichnevetsky, Editor, Advances in Computer Methods for Partial Differential Equations, AICA, Rutgers University Department of Computer Science, New Brunswick, N. J. (1975).

4. J. A. Meijerink and H. A. van der Vorst, "An Iterative Solution Method for Linear Systems of which the Coefficient Matrix is a Symmetric M-Matrix," Technical Report TR-1, Academic Computer Center, Budapestlaan 6, de Uithof-Utrecht, Netherlands (1976).

5. B. E. McDonald, T. P. Coffey, S. Ossakow, and R. N. Sudan, "Preliminary Report of Numerical Simulation of Type 2 Irregularities in the Equatorial Electrojet," J. Geophys. Res. 79, 2551 (1974).

6. B. E. McDonald, T. P. Coffey, S. Ossakow, and R. N. Sudan, "Numerical Studies of Type 2 Equatorial Electrojet Irregularity Development," Radio Science 10, 247 (1975).

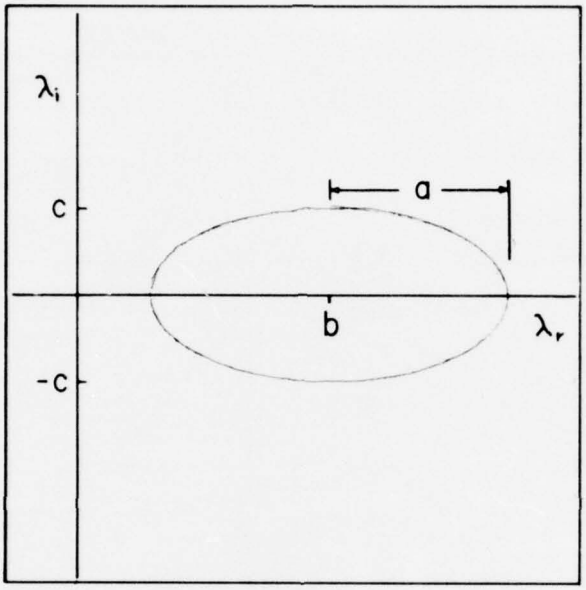

Fig. 1 — Ellipse containing complex eigenvalues

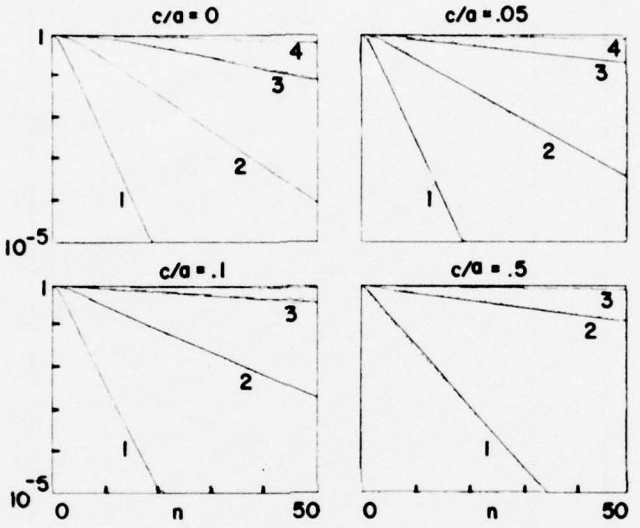

Fig. 2 — Error estimate E_n versus n.
Curves are labelled with $\log_{10}$ R.

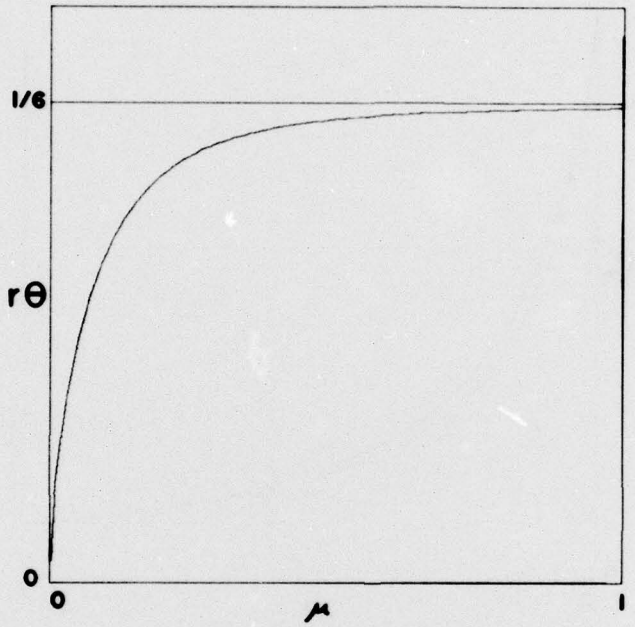

Fig. 3 — Optimal tuning parameter as determined from (68)

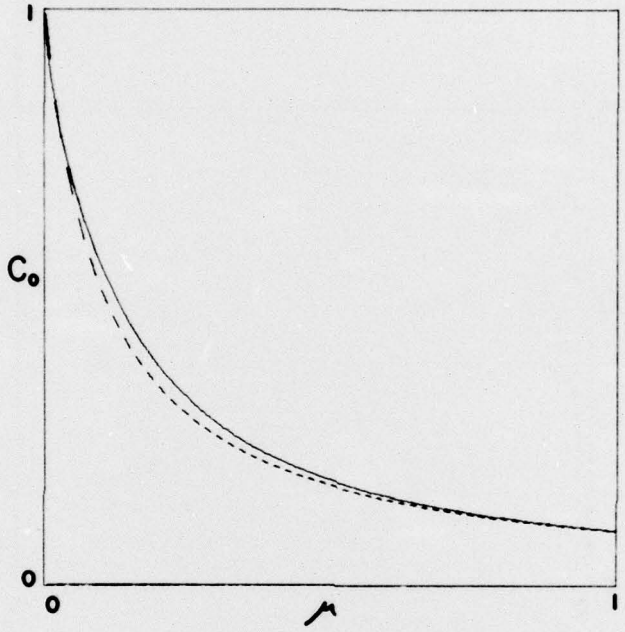

Fig. 4 — Normalized convergence rate (74) (solid); approximation (75) (dashed)

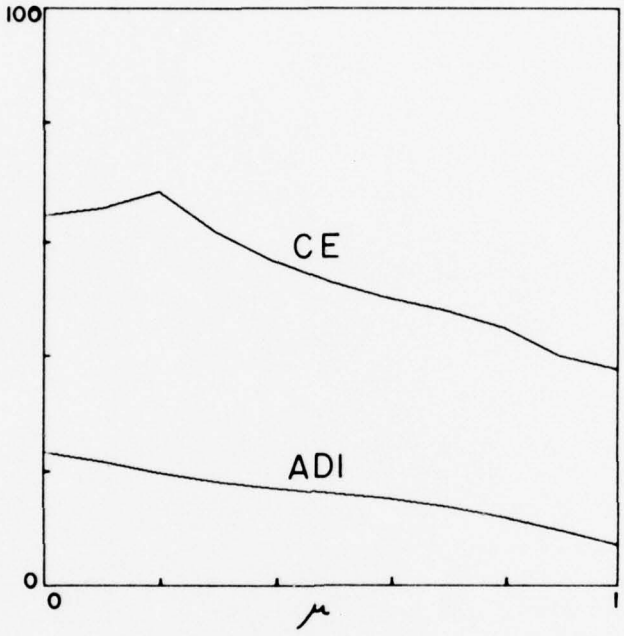

Fig. 5 — Computational efficiencies of the Chebychev explicit method (CE) and alternating direction implicit method (ADI) when applied to a series of numerical tests in which $|\underset{\sim}{A}|$ and thus μ vary from case to case. Plotted is the logarithm of the error reduction factor after many iterations, divided by the elapsed computer time in seconds.

DISTRIBUTION LIST

DIRECTOR
Defense Advanced Rsch Proj Agency
Architect Building
1400 Wilson Blvd.
Arlington, VA 22209
ATTN: Strategic Tech Office

Defense Communication Engineer Center
1860 Wiehle Avenue
Reston, VA 22090
ATTN: CODE R410 W. D. Dehart

DIRECTOR
Defense Communications Agency
Washington, D. C. 20305
ATTN: CODE 960
ATTN: CODE 480

Defense Documentation Center
Cameron Station
Alexandria, VA 22314 — 12 copies (if open publication)
ATTN: TC — 2 copies (if otherwise)

DIRECTOR
Defense Intelligence Agency
Washington, D. C. 20301
ATTN: W. Wittig DC-7D
ATTN: DT-1B

DIRECTOR
Defense Nuclear Agency
Washington, D. C. 20305
ATTN: STSI Archives
ATTN: STVL
ATTN: STTL Tech Library — 2 copies
ATTN: DDST
ATTN: RAAE — 3 copies

DIR OF DEFENSE RSCH & ENGINEERING
Washington, D. C. 20301
ATTN: DD/S&SS John B. Walsh
ATTN: OAD/EPS LTC W. A. Whitaker

COMMANDER
Field Command
Defense Nuclear Agency
Kirtland AFB, NM 87115
ATTN: FCPR
ATTN: FCPR COL. John P. Hill

Interservice Nuclear Weapons School
Kirtland AFB, NM 87115
ATTN: Document Control

DIRECTOR
Joint Strat TGT Planning Staff Jcs
Offutt AFB
Omaha, NB 68113
ATTN: JLTW-2
ATTN: JPST G. D. Burton
ATTN: JPST MAJ. J. S. Green

CHIEF
Livermore Division FLD Command DNA
Lawrence Livermore Laboratory
P. O. Box 808
Livermore, CA 94550
ATTN: FCPRL

COMMANDER
National Military Comd Sys Support Ctr
Pentagon
Washington, D. C. 20301
ATTN: B211
ATTN: DP Director for CSPO

OJCS/J-3
The Pentagon
Washington, D. C. 20301
ATTN: J-3 OPS ANAL BR. COL. Longsberry
ATTN: J-6

DIRECTOR
Telecommunications & Comd & Con Sys
Washington, D. C. 20301
ATTN: ASST DIR Info & Space Sys.
ATTN: DEP ASST. SEC Sys.

DIRECTOR
National Security Agency
Ft. George G. Meade, Md. 20755
ATTN: W14 Pat Clark
ATTN: Frank Leonard

Weapons Systems Evaluation Group
400 Army Navy Drive
Arlington, VA 22202
ATTN: DOCUMENT CONTROL

DIRECTOR
BMD Advanced Tech Ctr.
Huntsville Office
P. O. Box 1500
Huntsville, AL 35807
ATTN: ATC-T Melvin T. Capps

MANAGER
BMD Program Office
1300 Wilson Blvd.
Arlington, VA 22209
ATTN: Plans Division
ATTN: DACS-BMS Julian Davidson

COMMANDER
Harry Diamond Laboratories
2800 Powser Mill Road
Adelphi, Md. 20783
ATTN: AMXDO-NP

COMMANDER
TRASANA
White Sands Missle Range, NM 88002
ATTN: EAB

DIRECTOR
U.S. Army Ballistic Research Labs
Aberdeen Proving Ground, Md. 21003
ATTN: AM-CA Franklin E. Niles

U.S. Army Communications CMD
C-E Services Division
Pentagon Rm. 2d513
Washington, D. C. 20310
ATTN: CEAD

COMMANDER
U.S. Army Material Command
5001 Eisenhower Avenue
Alexandria, VA 22333
ATTN: AMCRD-WN-RE John F. Corrigan

Commander
U.S. Army Electronics Command
Fort Monmouth, N. J. 07703
ATTN: AMSEL-TL-ENV Hans A. Bomke

COMMANDER
U.S. Army Material Command
Foreign and Scientific Tech Center
220 7th St. N. E.
Charlottesville, VA 22901
ATTN: P. A. Crowley
ATTN: R. Jones

COMMANDER
U.S. Army Missile Command
Redstone Arsenal
Huntsville, AL 35809
ATTN: ASMI-YTT W. G. Preussel, Jr.

COMMANDER
U.S. Army Nuclear Agency
Fort Bliss, TX 79916
ATTN: CDINS-E
ATTN: USANUA-W. J. Berbert

CHIEF OF NAVAL RESEARCH
Department of the Navy
Arlington, VA 22217
ATTN: CODE 464 Jacob L. Warner
ATTN: CODE 464

COMMANDER
Naval Air Systems Command
Headquarters
Washington, D. C. 21350
ATTN: AIR 5381

COMMANDER
Naval Electronics Systems Command
Naval Electronics Systems CMD HQS
Washington, D. C. 20360
ATTN: NAVALEX 034 T. Barry Hughes
ATTN: PME 106-1 Satellite Comm Project Off
ATTN: John E. Doncarlos
ATTN: PME 117

COMMANDER
Naval Electronics Laboratory Center
San Diego, CA 92152
ATTN: William F. Moler
ATTN: CODE 2200 1 Verne E. Hildebrand
ATTN: R. Eastman

COMMANDING OFFICER
Naval Intelligence Support CTR
4301 Suitland Road, Bldg.5
Washington, D. C. 20390
ATTN: Mr. Dubbin Stic 12

DIRECTOR
Naval Research Laboratory
Washington, D. C. 20375
ATTN: HDQ COMM DIR Bruce Wald
ATTN: CODE 5460 Radio Propagation BR
ATTN: CODE 7127, Charles Y. Johnson
ATTN: CODE 7701, Jack D. Brown
ATTN: CODE 7700, Division Superintendent, 25 copies (if open publication)
1 copy (if otherwise)
ATTN: CODE 7750, Branch Head 150 copies (if open publication)
1 copy (if otherwise)

COMMANDING OFFICER
Naval Space Surveillance System
Dahlgren, VA 22448
ATTN: Capt. J. H. Burton

COMMANDER
Naval Surface Weapons Center
White Oak, Silver Spring, Md. 20910
ATTN: CODE 730 Tech. Lib.
ATTN: CODE 1224 Navy Nuc Prgms Off

DIRECTOR
Strategic Systems Project Office
Navy Department
Washington, D. C. 20376
ATTN: NSP-2141

COMMANDER
ADC/AD
ENT AFB CO 80912
ATTN: ADDA

AF Cambridge Rsch Labs, AFSC
L. G. Hanscom Field
Bedford, MA 01730
ATTN: LKB Kenneth S. W. Champion
ATTN: OPR Harvey P. Gauvin
ATTN: OPR James C. Ulwick

AF Weapons Laboratory, AFSC
Kirtland AFB, NM 87117
ATTN: DYT LT Mark A. Fry
ATTN: DYT CAPT Wittwer
ATTN: John M. Kamm SAS
ATTN: SUL

AFTAC
Patrick AFB, FL 32925
ATTN: TF MAJ. E. Hines
ATTN: TF/CAPT. Wiley
ATTN: TN

Air Force Avionics Laboratory, AFSC
Wright-Patterson AFB, OH 45433
ATTN: AFAL AVWE Wade T. Hunt

Assistant Chief of Staff
Studies and Analysis
Headquarters, U. S. Air Force
Washington, D. C. 20330

Headquarters
Electronic Systems Division, (AFSC)
L. G. Hanscom Field
Bedford, MA 01730
ATTN: XRE LT. Michaels
ATTN: LTC J. Morin CDEF XRC
ATTN: YSEV

COMMANDER
Foreign Technology Division, AFSC
Wright-Patterson AFB, OH 45433
ATTN: TD-BTA, LIBRARY

HQ, USAF/RD
Washington, D. C. 20330
ATTN: RDQ

COMMANDER
Rome Air Development Center, AFSC
Griffiss, AFB, N. U. 13440
ATTN: EMTLD Doc Library

COMMANDER IN CHIEF
Strategic Air Command
Offutt AFB, NB 68113
ATTN: XPFS MAJ. Brian G. Stephan

5441ES
Offutt AFB, NB 68113
ATTN: RDPO LT. Alan B. Merrill

Los Alamos Scientific Laboratory
P. O. Box 1663
Los Alamos, NM 87544
ATTN: DOC CON for Eric Lindman
ATTN: DOC CON for H. M. Peek
ATTN: DOC CON for R . F. Taschek

Sandia Laboratories
P. O. Box 5800
Albuquerque, NM 87115
ATTN: DOC CON for A. Dean Thronbrough
ATTN: DOC CON for W. D. Brown
ATTN: DOC CON for D. A. Dahlgren, ORG 1722
ATTN: DOC CON for J. P. Martin, ORG 1732

University of California
Lawrence Livermore Laboratory
P. O. Box 808
Livermore, CA 94550
ATTN: Tech Info Dept L-3

Department of Commerce
National Oceanic & Atmospheric Admin.
Environmental Research Laboratories
Boulder, CO 80302
ATTN: Jospeh H. Pope
ATTN: C. L. Rufenach

Department of Commerce
Office of Telecommunications
Institute for Telecom Science
Boulder, CO 80302
ATTN: Glenn Falcon
ATTN: William F. Utlaut
ATTN: G. Reed
ATTN: L. A. Berry

Department of Transportation
Transportation Rsch. System Center
Kendall Square
Cambridge, MA 02142
ATTN: TER G. Harowles

NASA
Goddard Space Flight Center
Greenbelt, MD 20771
ATTN: CODE 750 T. Golden

NASA
600 Independence Ave., S. W.
Washington, D. C. 20546
ATTN: M. Dubin

Aerospace Corporation
P. O. Box 92957
Los Angeles, CA 90009
ATTN: T. M. Salmi
ATTN: S. P. Bower
ATTN: V. Josephson
ATTN: SMFA for PWW

Analytical Systems Engineering Corporation
S Old Concord Rd.
Burlington, MA 08103
ATTN: Radio Sciences

Avco-Everett Research Laboratory, Inc.
2385 Reverse Beach Parkway
Everett, MA 02149
ATTN: Richard M. Patrick

Boeing Company, The
P. O. Box 3707
Seattle, WA 98124
ATTN: D. Murray
ATTN: Glen Keister

Brown Engineering Company, Inc.
Cummings Research Park
Huntsville, AL 35807
ATTN: David Lambert MS 18

California, University of - San Diego
Security Office 2-017
La Jolla, CA 92093

ATTN: Henry G. Booker

Calspan Corporation
P. O. Box [illegible] 5
Buffalo, N[illegible] 14221
ATTN: Romeo A. Deliberis

Computer Sciences Corporation
P. O. Box 530
6565 Arlington, VA 22046
ATTN: H. Blank

Comsat Laboratories
P. O. Box 115
Clarksburg, Md. 20734
ATTN: R. R. Taur

Cornell University
Department of Electrical Engineering
Ithaca, N. Y. 14850
ATTN: D. T. Farley, Jr.

ESL, INC.
495 Java Drive
Sunnyvale, CA 94086
ATTN: J. Roberts
ATTN: V. L.Mower
ATTN: James Marshall
ATTN: R. K. Stevens

General Electric Company
Tempo-Center for Advanced Studies
816 State Street
Santa Barbara, CA 93102
ATTN: Don Chandler
ATTN: DASIAC
ATTN: Tim Stephens

General Electric Company
P. O. Box 1122
Syracuse, N. Y. 13201
ATTN: F. A. Reibert

General Research Corporation
P. O. Box 3587
Santa Barbara, CA 93105
ATTN: John Ise, Jr.

Geophysical Institute
University of Alaska
Fairbanks, AK 99701
ATTN: Technical Library
ATTN: Neil Brown
ATTN: T. N. Davis

GTE Sylvania, Inc.
189 B Street
Needham Heights, MA 02194
ATTN: Marshal Cross

HRB-Singer, Inc.
Science Park, Science Park Road
P. O. Box 60
State College, PA 16801
ATTN: Larry Feathers

Illinois, University of
133 Davenport House
807 South Wright Street
Champaign, IL 61820
Attn: H. C. Yeh

Institute for Defense Analyses
400 Army-Navy Drive
Arlington, VA 22202
ATTN: Ernest Bauer
ATTN: Hans Wolfhard
ATTN: J. M. Aein
ATTN: Joel Bengston

Intl Tel & Telegraph Corporation
500 Washington Avenue
Nutley, N. J. 07110
ATTN: Technical Library

ITT Electro-Physics Laboratories, Inc.
9140 Old Annapolis Road
Columbia, MD. 21043
ATTN: John M. Kelso

John Hopkins University
Applied Physics Laboratory
8621 Georgia Avenue
Silver Spring, Md. 20910
ATTN: Document Librarian

Lockheed Missiles & Space Co., Inc.
P. O. Box 504
Sunnyvale, CA 94088
ATTN: Dept. 60-12

Lockheed Missiles and Space Company
3251 Hanover Street
Palo Alto, CA 94304
ATTN: Billy M. McCormac, Dept 52-14
ATTN: Martin Walt, Dept 52-10
ATTN: Richard G. Johnson, Dept 52-12

MIT Lincoln Laboratory
P. O. Box 73
Lexington, MA 02173
ATTN: Mr. Walden, X113
ATTN: D. Clark
ATTN: James H. Pannell L-246
ATTN: Lib A-082 for David M. Towle

Martin Marietta Corporation
Denver Distribution
P. O. Box 179
Denver, CO 80201
ATTN: Special Projects Program 248

Maxwell Laboratories, Inc.
9244 Balboa Avenue
San Diego, CA 92123
ATTN: A. J. Shannon
ATTN: V. Fargo
ATTN: A. N. Rostocker

McDonnell Douglas Corporation
5301 Bolsa Avenue
Huntington Beach, CA 92647
ATTN: J. Moule
ATTN: N. Harris
ATTN: Tech Library Services

Mission Research Corporation
735 State Street
Santa Barbara, CA 93101
ATTN: Ralph Kilb
ATTN: R. Hendrick
ATTN: Conrad L. Longmire
ATTN: R. E. Rosenthal
ATTN: R. Bogusch
ATTN: David Sowle
ATTN: M. Scheibe
ATTN: P. Fischer

Mitre Corporation, The
Route 52 and Middlesex Turnpike
P. O. Box 208
Bedford, MA 01730
ATTN: S. A. Morin M/S
ATTN: Chief Scientist W. Sen
ATTN: G. Harding

Mitre Corporation, The
Westgate Research Park
1820 Dolley Madison Blvd.
McLean, VA 22101
ATTN: Allen Schneider

North Carolina State Univ. at Raleigh
North Carolina State Univ. Campus
Raleigh, N. C. 27606
ATTN: SEC OFFICER for Walter A. Flood

Pacific-Sierra Research Corp.
1456 Cloverfield Blvd.
Santa Monica, CA 9-4-4
ATTN: E. C. Field, Jr.

Philco-Ford Corporation
Western Development Laboratories Div.
3939 Fabian Way
Palo Alto, CA 94303
ATTN: J. T. Mattingley MS X22

Photometrics, Inc.
443 Marrett Road
Lexington, MA 02173
ATTN: Irving L. Kofsky

Physical Dynamics, Inc.
P. O. Box 1069
Berkeley, CA 94701
ATTN: Joseph B. Workman

R & D Associates
P. O. Box 3580
Santa Monica, CA 90402
ATTN: Forest Gilmore
ATTN: Richard Latter
ATTN: Robert E. Lelevier
ATTN: William B. Wright, Jr.

Rand Corporation, The
1700 Main Street
Santa Monica, CA 90406
ATTN: Cullen Crain

Science Applications, Inc.
P. O. Box 2351
La Jolla, CA 92038
ATTN: Daniel A Hamlin
ATTN: D. Sachs
ATTN: E. A. Staraker

Stanford Research Institute
333 Ravenswood Avenue
Menlo Park, CA 94025
ATTN: L. L. Cobb
ATTN: Walter G. Chestnut
ATTN: Donald Neilson
ATTN: David A. Johnson
ATTN: Charles L. Rino
ATTN: E. J. Fremouw
ATTN: Dale H. Davis

TRW Systems Group
One Space Park
Redondo Beach, CA
ATTN: J. W. Lowry
ATTN: P. H. Katsos

Advanced Research Projects Agency (ARPA)
Strategic Technology Office
Arlington, Virginia

Capt. Donald M. LeVine

Naval Research Laboratory
Washington, D. C. 20375

Dr. P. Mange
Dr. E. Peterkin
Dr. R. Meier
Dr. E. Szuszczewicz -- Code 7127
Dr. Timothy Coffey -- Code 7700 (20 copies)
Dr. J. Goodman -- Code 7950

Science Applications, Inc.
1250 Prospect Plaza
La Jolla, California 92037

Dr. D. A. Hamlin
Dr. L. Linson
Dr. D. Sachs

Director of Space and Environmental Laboratory
NOAA
Boulder, Colorado 80302

Dr. A. Glenn Jean
Dr. G. W. Adams
Dr. D. N. Anderson
Dr. K. Davies
Dr. R. F. Donnelly

A. F. Cambridge Research Laboratories
L. G. Hanscom Field
Bedford, Mass. 01730

Dr. T. Elkins
Dr. W. Swider
Mrs. R. Sagalyn
Dr. J. M. Forbes
Dr. T. J. Keneshea

Office of Naval Research
800 North Quincy Street
Arlington, Virginia 22217

Dr. J. G. Dardis
Dr. H. Mullaney

Commander
Naval Electronics Laboratory Center
San Diego, California 92152

Dr. M. Bleiweiss
Dr. I. Rothmuller
Dr. V. Hildebrand
Mr. R. Rose

U. S. Army Aberdeen Research and Development Center
Ballistic Research Laboratory
Aberdeen, Maryland

Dr. F. Niles
Dr. J. Heimerl

Commander
Naval Air Systems Command
Department of the Navy
Washington, D. C. 20360

Dr. T. Czuba

Harvard University
Harvard Square
Cambridge, Mass.

Dr. M. B. McElroy
Dr. R. Lindzen

Pennsylvania State University
University Park, Pennsylvania 16802

Dr. J. S. Nisbet
Dr. P. R. Rohrbaugh
Dr. D. E. Baran
Dr. L. A. Carpenter
Dr. M. Lee
Dr. R. Divany
Dr. P. Bennett
Dr. E. Klevans

University of California, Los Angeles
405 Hillgard Avenue
La Jolla, California 90024

Dr. F. V. Coroniti
Dr. C. Kennel

University of California, San Diego
P. O. Box 109
La Jolla, California 92037

Dr. P. M. Banks

Utah State University
4th N. and 8th E. Streets
Logan, Utah 84322

Dr. R. Harris
Dr. V. Peterson
Dr. R. Megill

Cornell University
Ithaca, New York 14850

Dr. W. E. Swartz
Dr. R. Sudan
Dr. D. Farley
Dr. M. Kelley

NASA
Goddard Space Flight Center
Greenbelt, Maryland 20771

Dr. S. Chandra
Dr. K. Maedo

Princeton University
Plasma Physics Laboratory
Princeton, New Jersey 08540

Dr. F. Perkins

Institute for Defense Analysis
400 Army/Navy Drive
Arlington, Virginia 22202

Dr. E. Bauer

Director
Defense Nuclear Agency
Washington, D. C. 20305

Attn: G. K. Soper
Attn: Marvin Atkins